Available online at www.sciencedirect.com
SCIENCE DIRECT®
ELSEVIER
International Journal of Multiphase Flow 30 (2004) 311–325
International Journal of Multiphase Flow
www.elsevier.com/locate/ijmulflow

An experimental study of condensation heat transfer inside a mini-channel with a new measurement technique

Jeong Seob Shin, Moo Hwan Kim *

Department of Mechanical Engineering, Pohang University of Science and Technology, San 31, Hyoja-dong, Namgu, Pohang, Kyoungbuk 790-784, South Korea

Received 24 July 2003; received in revised form 23 December 2003

Abstract

New experimental techniques were developed to measure the in-tube condensation heat transfer coefficient. In this study, very low heat dissipation rates such as several watts from the mini-channel could be estimated and low mass flow rates below the 0.2 kg/h could be measured with reasonable uncertainties. To the authors' knowledge, these techniques provide a unique experimental apparatus for measuring the condensation heat transfer coefficients inside the sub-millimeter hydraulic diameter single channels. By careful design and construction of the experimental apparatus, the characteristics of the local heat transfer and pressure drop were experimentally investigated using the condensing R134a two-phase flow, in a horizontal single round tube, with an inner diameter of 0.691 mm. Tests were performed for a mass flux of 100–600 kg/m^{2}s, a heat flux of 5–20 kW/m^2, and a saturation temperature of 40 °C. The experimental data of the Nusselt number and two-phase frictional pressure gradient are presented and compared with the existing correlations.

Keywords: Two-phase flow; Condensation; Heat Transfer; In-tube; Mini-channel

1. Introduction

Small hydraulic diameter tubes are widely used in residential and automotive air-conditioners. Many of these tubes are made from copper and multi-port extruded aluminum. New applications in the field of micro-electronics are another growing issue. Hence, prediction of the condensation heat transfer coefficient and the pressure drop across small tubes is of great interest. It is difficult,

* Corresponding author. Tel.: +82-54-279-2165; fax.: +82-54-279-3199.
E-mail address: mhkim@postech.ac.kr (M.H. Kim).

0301-9322/$ - see front matter
doi:10.1016/j.ijmultiphaseflow.2003.11.012

however, to apply data for large tubes to small tubes, because there are many differences in the relative magnitudes of gravity, shear, and surface tension forces, all of which determine the characteristics of the condensation heat transfer and pressure drop.

With traditional experimental methods such as the secondary fluid (e.g., water) calorimetric method, it is difficult to accurately test the local condensation heat transfer inside mini-channels. Hence, there are large discrepancies between the results of previous studies. The experimental methods as well as unidentified sources of uncertainties could be reasons for such discrepancies. However, those uncertainties have been largely overlooked in the literature. Guo and Li (2003) and Kandlikar (2003) addressed the importance of various sources of errors and a number of issues related to experimental errors associated with micro-channel flows.

Garimellar (2003) presented an experimental technique using an additional secondary refrigerant loop for the measurement of low heat transfer rates over small decrements of refrigerant quality and high heat transfer coefficient characteristics of the multi-port channels. This technique resulted in uncertainties typically as low as ±2% in the measurement of the secondary loop heat duty, at heat transfer rates less than 200 W. However, to test the condensation heat transfer inside the sub-millimeter hydraulic diameter single channels, very low heat flows such as several watts for the test section and low mass flows below the 0.2 kg/h should be controlled. There are problems in controlling those flow conditions, such as heat flux, mass flux, quality, etc. Heat losses in the small-scale heat transfer are another major source of inaccuracy. Hence, previous work usually used multi-port extruded rectangular channels as a test tube and most of the experimental work has been carried out by a so-called Wilson plot technique (1915). However, in the case of multi-port channels, the uniformity of the cross-section dimensions along the channel flow length and the channel-to-channel flow uniformity are significant (Kandlikar, 2003). In addition, the flow rate fluctuation effects (due to flow instabilities) on the heat transfer and pressure drop in multi-port channels may be different to those in a single tube. Kandlikar (2002) observed these flow instabilities in the multi-channel evaporators. In his previous evaporation study (Kandlikar et al., 2001), complete flow reversal was observed in some of the channels.

There have been very few previous attempts at measuring the condensation heat transfer coefficients inside the sub-millimeter-scale hydraulic diameter channels, even in the multi-port channels. Heun (1995) measured the R134a condensation data for multi-port flat extruded tubes with different cross-section shapes and hydraulic diameters in the range 0.6 mm $< D_h <$ 1.5 mm. The cross-section shapes were circles, squares, triangles, enhanced squares, and small squares. They concluded that Dobson (1994) correlation could predict the experimental data satisfactorily. Their apparatus used an air-to-refrigerant cross-flow heat exchanger as a test section.

Webb and Ermis (2001) investigated the effect of hydraulic diameter on the condensation coefficient and pressure drop using R134a. They used smooth and grooved rectangular multi-port flat extruded aluminum tubes with hydraulic diameters of 0.44, 0.611, 1.33, and 1.564 mm. The heat transfer to all of the tubes was reasonably well predicted by either the Akers et al. (1959) or the Moser et al. (1998) equivalent Reynolds number models.

Koyama et al. (2003) performed flow condensation experiments using R134a in four kinds of multi-port flat extruded aluminum tubes with rectangular cross-sections of about 1 mm in hydraulic diameter: an 8-channel 1.062 mm hydraulic diameter plain tube, a 19-channel 0.807 mm hydraulic diameter plain tube, an 8-channel 0.889 mm hydraulic diameter micro-finned tube, and an 8-channel 0.937 mm hydraulic diameter micro-finned tube. Their mass flux ranged from 100 to

700 kg/m^{2}s, quality ranged from 0.0 to 1.0 at a constant inlet pressure of 1.7 MPa. They compared frictional pressure drop and local heat transfer characteristics with previous correlations proposed for relatively large diameter tubes. In the cases of plain tubes, the experimental data for the frictional pressure drop were in good agreement with the Friedel (1979) correlation. Condensation heat transfer data (except for the cases of low mass velocity) was relatively in good agreement with the correlations supposed by Moser et al. (1998). Considering the effects of the surface tension and kinematic viscosity, Koyama et al. proposed new correlations of the frictional pressure drop and in-tube condensation heat transfer coefficient.

Kim (1996) investigated the condensation of R12 and R134a in nine multi-port flat extruded aluminum tubes with rectangular cross-sections of 16 mm in width and 1.7 mm in height. The experimental tubes were separated into 8–23 parallel channels by membranes. The hydraulic diameters ranged from 0.717 to 1.171 mm. Kim reported that the condensation heat transfer rate increased with the number of channels because the heat transfer area also increased. The pressure drop increased with the mass flux, especially for the case with 23 channels. The heat transfer rate initially increased with the number of fins, but for more than four fins, the heat transfer rate decreased, due to the inundation of the condensate liquid.

In this study, totally new experimental techniques were developed to measure the in-tube condensation heat transfer coefficient. With these techniques, very low heat dissipation rate and mass flow rate could be measured with reasonable uncertainties. To the authors' knowledge, these techniques provide a unique experimental apparatus for measuring the condensation heat transfer coefficients inside sub-millimeter hydraulic diameter single channels. Using this experimental apparatus, the condensation heat transfer coefficients of R134a inside a horizontal round tube, with an inner diameter of 0.691 mm, at a saturation temperature of 40 °C were measured. The condensation Nusselt numbers and two-phase frictional pressure gradients are presented and compared with existing correlations.

2. Measurement techniques

2.1. In-tube condensation heat transfer coefficient

With the conventional test methods, it is very difficult to measure the small scale in-tube condensation heat transfer coefficient accurately. The test tube size and refrigerant flow rate were too small to measure the condensation heat transfer coefficient directly without introducing a large error. In the present study, new techniques were developed for the measurement of condensation heat transfer inside the single tubes.

A conceptual schematic diagram of the measurement technique is depicted in Fig. 1. In this figure, T_w is the average wall temperature of the test tube outer surface, T_{sr} is the average surface temperature of the refrigerant tube side fin, and T_{sh} is the average surface temperature of the heater tube side fin. The test section consisted of round copper tubes, a heater wire, an air duct, and fans. An identical copper tube was attached to each fin. The refrigerant flowed horizontally into one tube (the lower tube in Fig. 1) and a heater wire was inserted into the other tube (the upper tube in Fig. 1). These fin and tube sets were mounted parallel to the cross-flow air duct. The fan and heater wire were connected to variable DC power supplies. If the two average

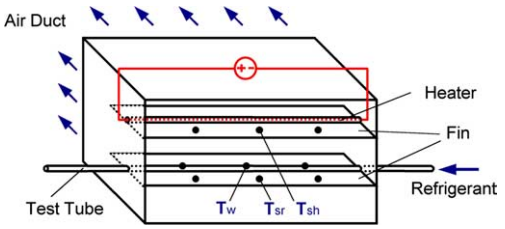

Fig. 1. Conceptual schematic diagram of the test section.

temperatures (i.e., T_{sh} and T_{sr}) at identical locations on the two fin surfaces were the same, then the heat removal from the refrigerant tube and the heater tube would be also the same. However under actual test conditions, it is difficult to make these average surface temperatures exactly the same. Hence, following equations are used to estimate heat dissipation rate accurately even though there is a small temperature difference (<0.5 °C) between two surfaces.

Heat transfer rate of each fin surfaces can be expressed like Eqs. (1) and (2).

$$\dot{Q}_{heater} = h_{sh}A_{sh}(T_{sh} - T_{amb}) \tag{1}$$

$$\dot{Q}_{estimation} = h_{sr}A_{sr}(T_{sr} - T_{amb}) \tag{2}$$

where $\dot{Q}_{heater}$ is the power input of the heater tube, h_s is the airside average heat transfer coefficient of the fin surface, A_s is the fin surface area, T_{amb} is the ambient air temperature, $\dot{Q}_{estimation}$ is the estimated heat dissipation rate of the test tube, and the subscripts 'h' and 'r' refer to heater tube side fin and refrigerant tube side, respectively. With this identical geometry of the test section, two surfaces have the same area (i.e., $A_{sh} = A_{sr}$). And with the similar fin surface temperatures, airside heat transfer coefficients of both fins would be almost same (i.e., $h_{sh} = h_{sr}$). Then, heat dissipation rate could be estimated using Eq. (3)

$$\dot{Q}_{estimation} = \frac{T_{sr} - T_{amb}}{T_{sh} - T_{amb}}\dot{Q}_{heater} \tag{3}$$

The rate of heat dissipation (or heat flux in the test section) was controlled by varying the revolutions per minute of the fan. Information about both the flow rate and temperature difference of the secondary fluid (i.e., air) was not required. From this concept, the heat flux was easily controlled and measured. A heat loss problem did not exist in the test section, so no insulation was required. Since short test section length could be used, it was possible to test with the low heat transfer rates condition such as small decrements of the refrigerant quality. In addition, short test section made more uniform fin surface temperature along the test tube, and then more accurate measurement was possible. In this test, maximum fin surface temperature change along the measurement locations was about ±0.8 °C.

2.1.1. Test section

Fig. 2 shows photography of the cross-flow air-cooled test section and the locations of thermocouples installation. The test section had an effective length of 171 mm, and the smooth round

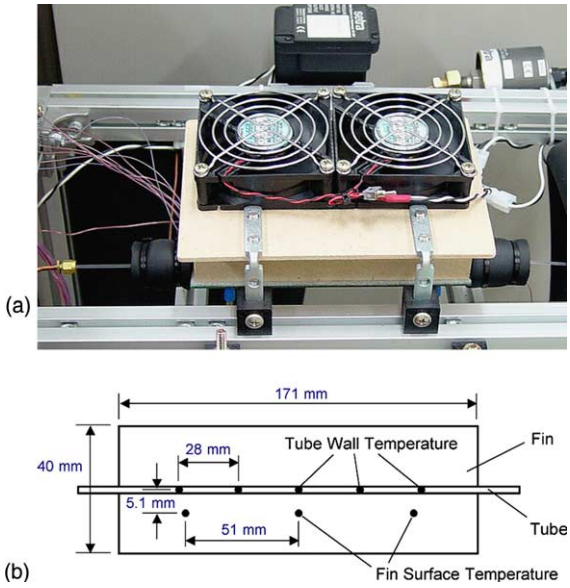

Fig. 2. Cross-flow air-cooled test section: (a) photograph of the test section and (b) locations of thermocouples installation.

copper test tube had a 0.691 mm inner diameter. A material of the fin surface is a copper. A variable DC power supply was connected to the wire heater to measure the heat flux of the test section. Straight nichrome wire of uniform diameter was used as a heater. Six T-type thermocouples were soldered onto the outer surface (three for top and three for bottom) of the test tube at 28 mm intervals to measure the tube surface temperatures. Two sets of three thermocouples were attached to each fin surface to measure the average fin surface temperature. Prior to installation of the test section, the preliminary test was conducted to find the proper measurement locations of the fin surface temperatures. As a result, Fig. 2(b) shows temperature measurement locations of the test tube. With these locations, reasonable fin surface temperatures were obtained. The refrigerant side saturation temperature was estimated from the measured pressure. To avoid any gravitational effects on the pressure and pressure drop measurements, pressure transducers and transducer ports were positioned parallel to the test tube so that both were in the same horizontal plane. The pressures were measured 20 mm before the inlet, and after the outlet, of the test tube.

Prior to measuring the condensation heat transfer coefficients, verification of this test section is required. To do this, instead of flowing refrigerant in the test section, another heater wire was inserted in the refrigerant side tube and DC power was supplied. Average fin surface temperatures were measured and the heat dissipation rate from the test section was estimated according to Eq. (3). Comparing results of this estimated heat dissipation rate with actual heater input power is shown in Fig. 3. It shows reasonable results with a maximum error of 2.6% and standard deviation of 1.4%. As shown in this figure, this test section made the measurement of very small heat dissipation rates such as 0.75 W possible.

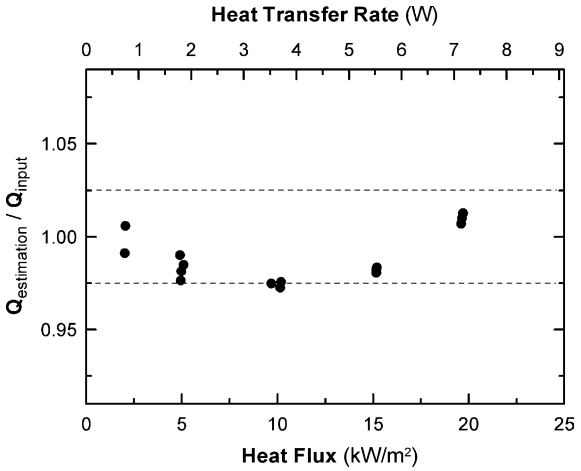

Fig. 3. Preliminary test result of the test section.

2.2. Mass flow rate

To measure the condensation heat transfer inside the sub-millimeter tubes, very small mass flow rates (such as below 0.2 kg/h) and a wide range of the mass flows should be measured accurately. However, there is little information on how to measure mass flows in this range.

In front of the refrigerant circulation pump, the receiver is generally used to supply liquid for the pump. Mass of the liquid in the receiver can be measured by determining the pressure at the bottom of the receiver. The measurement apparatus for the mass flow rate in the receiver is shown in Fig. 4. This receiver consisted of two identical tanks, two transparent tubes, two valves, and a differential pressure transducer. The valves in the receiver tanks were all opened during normal operation. The refrigerant liquid levels of the receiver tanks were equalized and stabilized during steady-state conditions. When the lower valve of the receiver was closed, the liquid level of the right tank decreased, and that of the left tank increased. A pre-calibrated differential pressure transducer (Druck LPM 9481, variable inductance type, 0–2000 Pa, ±0.1% of the full scale) read

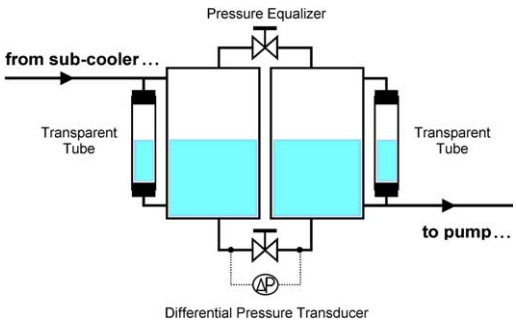

Fig. 4. Schematic of the mass flow meter.

the differential pressure gradient between the two tanks; this reading was converted to the mass flow rate as shown in Eq. (6)

$$\Delta p = \rho g \Delta h \tag{4}$$

$$\Delta m = \rho \frac{\Delta h}{2} A = \frac{\Delta p}{2g} A \tag{5}$$

$$\dot{m} = \frac{\Delta m}{\Delta t} \tag{6}$$

where Δp is the pressure difference at the bottom of the two tanks, ρ is the density of the refrigerant liquid, g is the gravitational acceleration, Δh is the liquid level difference of the two tanks, Δm is the mass of the refrigerant flows during time Δt, and A is the inside cross-sectional area of each tank.

Owing to the use of two tanks, it is possible to feed liquid into the pump while measuring pressure, the sensitivity of the pressure measurement is doubled compared to that of a single tank. Schnell (1997) introduced this measurement technique for very small liquid flows; below 0.2 l/h. But with his device, it is difficult to accurately measure the mass flow rate of the liquid in the saturation state. In most operating conditions, because of the sub-cooled liquid entering at the left tank, pressure of the left tank is slightly lower than that of the right tank. For example, a temperature difference of 0.01 °C for saturated R134a at 40 °C means a saturation pressure difference of about 270 Pa. This pressure difference can induces backflow in the pressure equalizer pipe between the tanks, this mass flow rate should be considered.

When the lower valve of the receiver tanks shown in Fig. 4 was opened and the upper valve closed, the liquid level change rate of the tanks approximately represents the backflow rate. By converting this liquid level change rate to vapor volume change rate, backflow rate can be estimated.

This flow rate measuring device has several advantages: measuring range can be easily changed by replacing receiver tanks, no contamination problems, and there is almost no additional pressure loss. Using this technique, mass flows below the 0.2 kg/h could be measured. Fig. 5 shows the measured result of the R134a mass flow rate at 0.138 kg/h (= 2.3 g/min), with the before mentioned device. Twenty data were recorded with 1.0 s intervals and the straight line means slope of the pressure difference change. It shows linear and stable results.

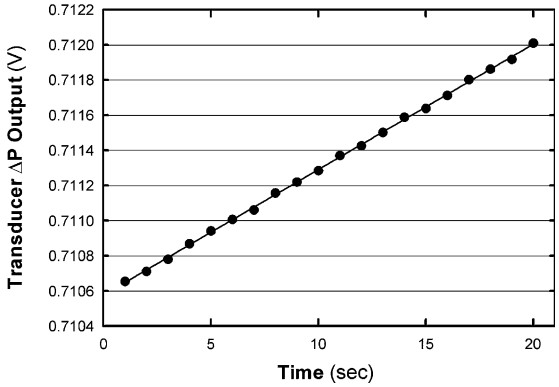

Fig. 5. Measurement result of the R134a mass flow rate at 0.138 kg/h (= 2.3 g/min).

2.3. Average inner diameter

As hydraulic diameter decreases, accurate information about cross-sectional dimensions becomes significant. Owing to the difficulties in measuring small dimension, manufacturer's specification was usually used. However any difference with the actual dimension may induce large uncertainties in measurement.

Direct measurement of the cross-section dimension is not easy because the tubes have no uniform cross-section and it is difficult to cut tubes without burrs or distortion. Hence, an indirect technique for the measurement of the average inner diameter of the tube is used. If the density of the tube material is known, the average inner diameter of the tube can be calculated using the tube average outer diameter, length, and mass as shown in Eq. (7).

$$\frac{D_o^2 - D_i^2}{D_o^2} = \frac{M_{tube}}{\rho\left(\frac{\pi D_o^2}{4} L\right)} \tag{7}$$

where M_{tube} is the mass of the tube, ρ is the density of the tube material, L is the length of the tube, and the subscripts 'o' and 'i' refer to outer and inner, respectively.

2.4. Heat loss in the pre-heater

With these new measurement techniques for the condensation heat transfer coefficient, a heat loss problem in the test section does not occur inherently. However, the heat loss problem in the pre-heater still exists. In this small-scale heat transfer test, heat balance estimation is very significant. Without accurate information about net heat input in the pre-heater, it is impossible to control inlet conditions for the test section. Hence, the reduction of heat loss as well as the accurate estimation of heat loss are both very significant.

In the pre-heater, a heater wire is inserted into the refrigerant tube instead of being wound onto the tube. Since maximum surface temperature of the pre-heater tube was limited by the saturation temperature of the refrigerant, heat loss was reduced greatly and was not changed largely according to the operating condition. In addition, if surface temperature of the refrigerant tube becomes saturation temperature without refrigerant flowing, then power input of the heater is same as heat loss. By this principle, calculated heat loss using one dimensional cylindrical coordinate conduction equation can be verified within maximum 10% accuracy. As a result, uncertainty in the test section inlet quality at lowest mass flux condition is estimated as ±0.05.

3. Experiment

3.1. Experimental apparatus

By using the mentioned measurement techniques, the experimental apparatus was constructed. The apparatus consisted of a circulation loop for the refrigerant, a water-cooled condenser, and a data acquisition system. Fig. 6 shows a schematic diagram of the test apparatus except the data acquisition system. The refrigerant circulation loop included a gear pump, a pre-heater, a test

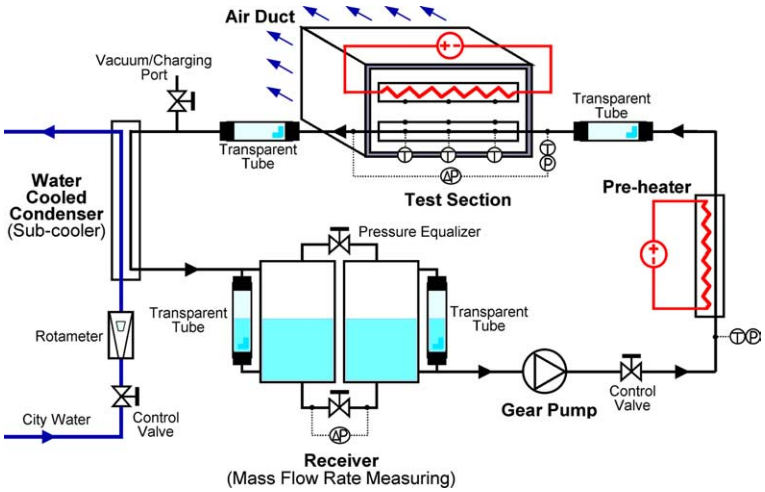

Fig. 6. Schematic diagram of the test apparatus.

section, a sub-cooling unit, and receivers. The R134a refrigerant was delivered to the test section by a variable speed magnetic gear pump. The control valve could further adjust the refrigerant flow. The refrigerant flow rate was measured using a differential pressure transducer installed between the two receiver tanks. The electric pre-heater regulated the refrigerant quality at the inlet of the test section. As described, to reduce the heat loss of the pre-heater, and to estimate its value accurately, a heater wire was inserted inside the refrigerant tube. The cooling air flowing in the duct of the test section condensed the refrigerant. Transparent Teflon tubes with a 0.75 mm inner diameter were installed at the inlet and outlet of the test section. The water-cooled condenser (i.e., sub-cooler) was used to cool the fluid exiting the test section. After condensation, the liquid refrigerant flowed back to the receiver. The operating pressure in the refrigerant loop was largely controlled by the receivers, using attached strip heaters. Adjusting the heater power set the desired temperature of the receivers and thus the loop operating pressure. The thermocouples were calibrated prior to their installation to an accuracy of ±0.1 °C.

3.2. Test conditions and methods

The experimental ranges are summarized in Table 1. Pure refrigerant R134a was used as the test fluid. The tests were conducted for condensation at a 100, 200, 400, or 600 kg/m^2 s mass flux. The

Table 1
Experimental conditions

Inner diameter	0.691 mm
Test section length	171 mm
Refrigerant	R134a
Condensation temperature	40 °C
Mass flux	100, 200, 400, 600 kg/m^{2}s
Heat flux	5, 10, 15, 20 kW/m^2
Quality range	About 0.15–0.85

mass flow rate for this range was 2.3–13.5 g/min. Regulating the input power of the variable speed magnetic gear pump changed the refrigerant flow rate in the tube. A constant heat flux of 5, 10, 15, or 20 kW/m^2, based on the inside tube surface area, was maintained throughout each test. The quality of the refrigerant entering the test section was controlled using the heater power of the pre-heater, and the heat flux was maintained by modulating the power of the test section fan.

3.3. Data acquisition

The test data was collected using a data acquisition system consisting of a data logger (Agilent 34970A), interface card (HPIB), and a compatible personal computer. The data was analyzed in real time using a PC and a data reduction program (MS-Excel with a Visual Basic). All of the information about the test conditions and test data were displayed on the monitor during the test, the test conditions were changed, based on this information.

The average heat transfer coefficient was obtained from the average value of the integral of the local heat transfer coefficient. For averaging, 20 data points were collected during 120 s. The heat transfer coefficients and the pressure drops were fitted over a quality range from 0.15 to 0.85. The thermodynamic and transport properties of R134a were calculated using REFPROP 5.1 (Huber et al., 1996).

3.4. Data reduction

3.4.1. Condensation heat transfer coefficient

The average qualities of the refrigerant at the inlet and test section were calculated from the energy balance in the pre-heater and the test section, respectively

$$x_{\mathrm{in}} = \frac{1}{i_{\mathrm{fg}}}\left[i_{\mathrm{ph,in}} + \frac{(\dot{Q}_{\mathrm{ph}} - \dot{Q}_{\mathrm{ph,loss}})}{\dot{m}_{\mathrm{r}}} - i_{\mathrm{f}}\right] \tag{8}$$

$$x = x_{\mathrm{in}} + \frac{\dot{Q}_{\mathrm{test}}}{2\dot{m}_{\mathrm{r}} i_{\mathrm{fg}}} \tag{9}$$

where x is the quality, i is the specific enthalpy, the subscripts 'in', 'ph', 'test', 'r', 'f', and 'g' means the inlet of the test tube, the pre-heater, the test tube, refrigerant, liquid, and gas, respectively. Here, the heat loss through the insulating foam of the pre-heater, $\dot{Q}_{\mathrm{ph,loss}}$ was calculated from the one-dimensional cylindrical conduction equation. The pre-heater was divided into the two sections (sub-cooled and two-phase) and the heat loss from the each section was estimated, respectively.

The condensation heat transfer coefficient and Nusselt number were calculated according to

$$h = \frac{q''}{T_{\mathrm{w}} - T_{\mathrm{r}}} \tag{10}$$

$$Nu = \frac{hD}{k_{\mathrm{f}}} \tag{11}$$

where h is the heat transfer coefficient, q'' is the heat flux, Nu is the Nusselt number, D is the inner diameter of the test tube, k_f is the thermal conductivity of the refrigerant liquid, and T_w and T_r are the average temperatures of the inside tube wall and the refrigerant, respectively. The heat flux was determined using the inside tube wall area and total heat dissipation rate in the test section. T_w was calculated from the temperatures measured at the outside tube wall using the one-dimensional cylindrical conduction equation.

3.4.2. Two-phase frictional pressure drop

The pressure drop between the inlet and outlet of the test section was measured using a differential pressure transducer. The overall pressure drop (measured in horizontal two-phase flow, Δp_{exp}) consisted of four components: the two-phase friction pressure drop (Δp_f), test section inlet pressure drop (Δp_{in}), test section outlet pressure change (Δp_{out}), and acceleration pressure change (Δp_{acc})

$$\Delta p_{exp} = \Delta p_f + \Delta p_{in} + \Delta p_{out} + \Delta p_{acc} \tag{12}$$

The inlet, outlet, and acceleration pressure changes were calculated using Eqs. (3.58), (3.50), and (2.31) of Collier and Thome (1994). In the present experiment, the friction pressure drop was 92–117% of the total experimental pressure drop depending on the operating conditions.

In most previous studies, average temperature of the refrigerant in the test section was obtained simply by averaging inlet temperature and outlet temperature of the test tube. However, as the hydraulic diameter decreased, inlet sudden contraction (i.e., ΔP_{in}) effect becomes so large. Without considering this effect, several percent errors in the heat transfer coefficient would be induced. Hence, instead of using inlet and outlet temperatures, average refrigerant temperature was estimated from average pressure of the test tube. By using Eq. (12), average saturation pressure of the test tube was obtained and then average saturation temperature was estimated from this value. Prior to installation, the relation between pressure transducer and temperature sensor was checked using preliminary test.

3.5. Experimental uncertainties

Table 2 shows estimated experimental uncertainties using the method by Holman (2001). Accounting for all of the instrument errors, the uncertainties for the average heat transfer coefficient were estimated at ±3.5 (condition for lowest mass flux, highest heat flux, and lowest quality) to ±19.9% (condition for highest mass flux, lowest heat flux, and highest quality).

4. Results and discussion

4.1. Condensation heat transfer

Fig. 7 gives the local condensation heat transfer behavior with the refrigerant quality and mass flux. Where G is the mass flux of the refrigerant. The Nusselt numbers calculated from Shah (1979) and Akers et al. (1959) are also shown in the figure. The local Nusselt number increased with the refrigerant quality, as expected, except for low mass fluxes. The Nusselt number became

Table 2
Experimental uncertainties

Temperature	±0.1 °C
Pressure	±1.5 kPa
Pressure difference (test section)	±0.15 kPa
Pressure difference (receiver)	±2 Pa
Mass flux	±3.5%
Heat flux	±3.2%
Heat transfer coefficient	±3.5 to ±19.9%

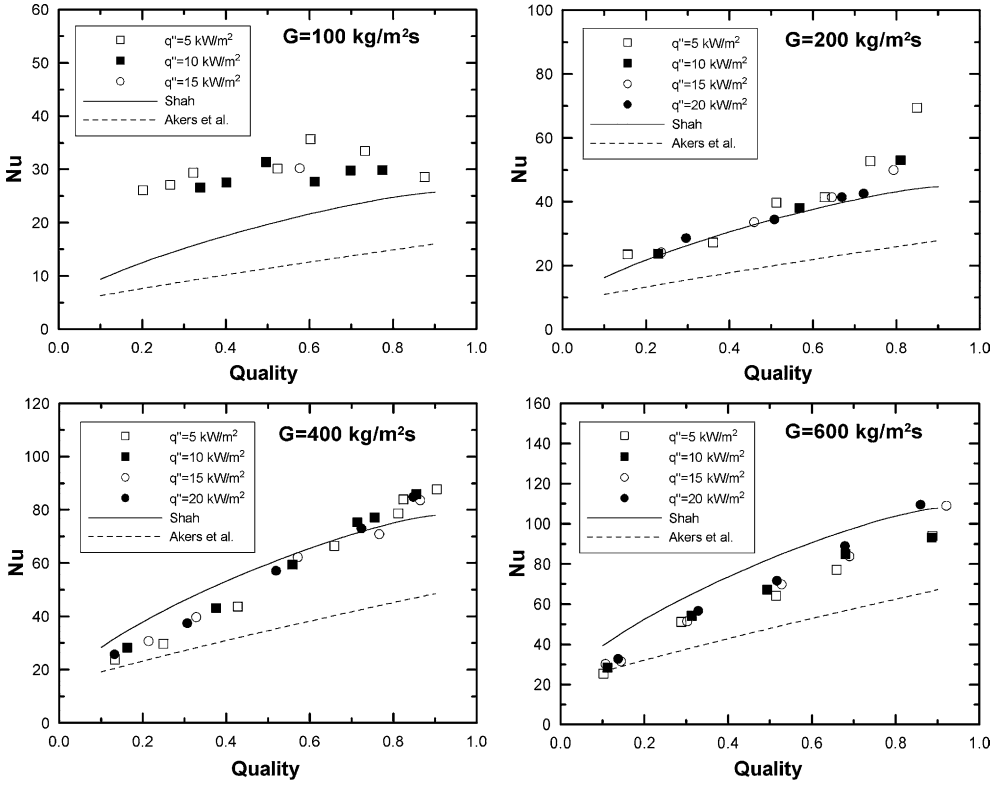

Fig. 7. Local Nusselt number.

more sensitive to the mass flux as the average quality increased. The same behavior was reported by Wang et al. (2002) for R134a using multi-port extruded rectangular channels with hydraulic diameters of 1.46 mm and a mass flux ranging between 75 and 750 kg/m^{2}s.

The effect of heat flux on condensation heat transfer was discussed in several previous studies (Yan and Lin, 1999; Yang and Webb, 1996). However, in this study, no evident relationship between the heat flux and condensation heat transfer was found.

Shah correlation gives good agreement in mass flux 200–600 kg/m^2. However, it also under predicts heat transfer coefficient in the low mass flux condition and over predicts in the high mass flux condition. Recent studies (Webb and Ermis, 2001; Wang et al., 2002; Yang and Webb, 1996;

Kim et al., 1997) for the condensation heat transfer inside the small hydraulic diameters presented that Akers et al. correlation predicted well with their results. In these experiments, Akers et al. correlation under predicted in all regions. However, its discrepancies decreased as mass flux increased.

It is inferred that flow pattern plays an important role in discrepancies between the experimental results and predicted values of the correlations. From the flow observation at the outlet of the test tube, stratified flow was not observed for all flow conditions in this small diameter tube. More accurate heat transfer predictions require a flow visualization approach during condensation heat transfer.

4.2. Two-phase pressure gradient

Fig. 8 gives the two-phase frictional pressure gradient results as functions of the refrigerant quality and mass flow rate. The pressure gradients calculated from Friedel (1979) correlation are also shown in the figure. No relationship between the heat flux and pressure drop was found. As would be expected, the local pressure drops increased with quality. However, the incremental rate decreased above a certain quality, depending on the mass flow rate. For a low mass flux (100 kg/m^2s), the incremental rate decreased above a quality of 0.6; for a mass flux of 400 kg/m^2s, the

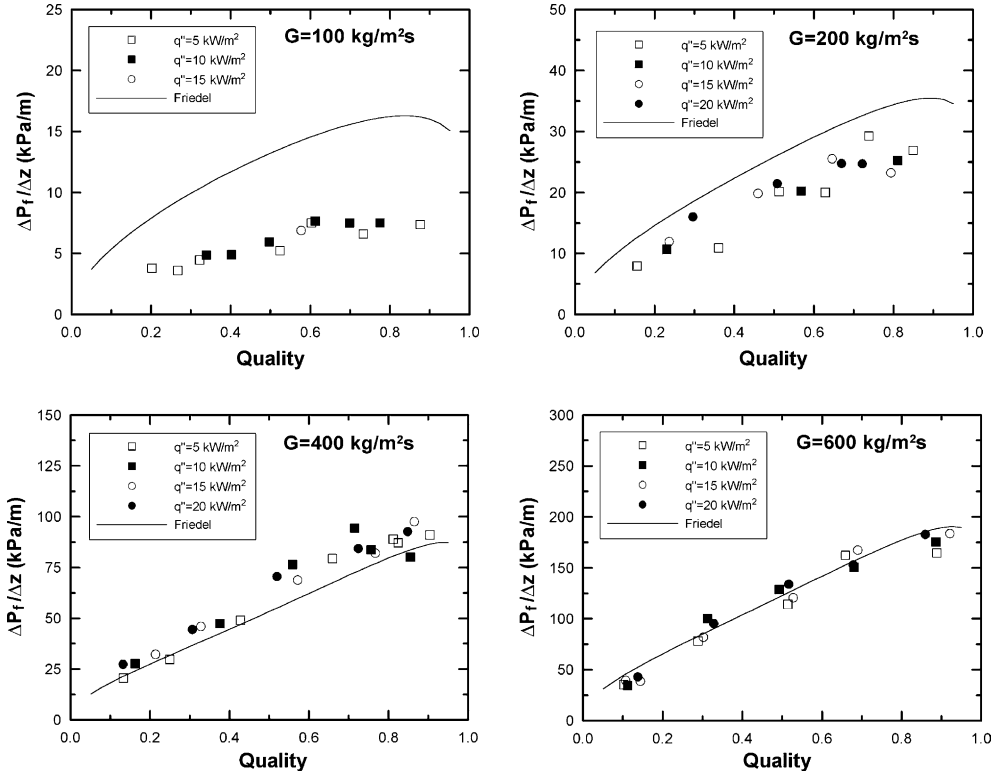

Fig. 8. Two-phase frictional pressure gradient.

incremental rate decreased above a quality of 0.7. As the quality or mass flux increased and the liquid layer became thinner, the roughness of the liquid–vapor interface decreased and therefore the pressure drop decreased (Christoffersen et al., 1993). This flow characteristic was verified by flow pattern observations at the outlet of the test tube.

Friedel correlation gives good agreement in high mass flux condition and over predicts pressure gradient in low mass flux condition. In the experiment, the pressure drop fluctuations were large, except for high quality flow. The effects of surface tension in the flow patterns probably contribute to these large fluctuations in the pressure drop. Since, average refrigerant temperature of the test section is estimated from average refrigerant pressure, heat transfer coefficients are also influenced by these large fluctuations.

5. Conclusions

Unique experimental techniques and test sections were developed to permit accurate measurements of the flow condensation coefficient and mass flux in a mini-channel. It is believed that by using these techniques, more fundamental studies for condensation heat transfer inside the mini-channel will be possible.

The condensation heat transfer and pressure drop characteristics of R134a in a small diameter single round tube were investigated by using newly developed experimental apparatus. The following main conclusions can be drawn from this experimental study:

- The Nusselt number and pressure gradient increased with the refrigerant mass flux.
- The Nusselt number and pressure gradient increased with the refrigerant quality, especially for high mass fluxes.
- No evident effect of the heat flux was found in the heat transfer coefficients and frictional pressure drop.
- Large pressure drop fluctuations were noted, except in the high quality flow range. Heat transfer coefficients were influenced by these fluctuations.
- Comparisons of experimental data with existing heat transfer correlations reveal that both the Shah (1979) and the Akers et al. (1959) correlations failed to predict the present data.
- Friedel (1979) correlation for pressure gradient gives good agreement in the high mass flux region. However, this correlation failed to predict the present data at lower mass flux.

Acknowledgements

This work was supported by the Ministry of Science and Technology of Korea through the National Research Laboratory program.

References

Akers, W.W., Deans, H.A., Crosser, O.K., 1959. Condensation heat transfer within horizontal tubes. Chemical Engineering Progress Symposium Series 55, 171–176.

Christoffersen, B.R., Chato., J.C., Wattelet, J.P., Souza, A.L., 1993. Heat transfer and flow characteristics of R22, R32/R125, and R134a in smooth and microfin tubes. ACRC Technical Report, vol. 47. University of Illinois at Urbana-Champaign, Urbana, IL.

Collier, J.G., Thome, J.R., 1994. Convective Boiling and Condensation, third ed. Oxford University Press, Oxford, UK.

Dobson, M.K., 1994. Heat transfer and flow regimes during condensation in horizontal tubes. Ph.D. Thesis, Univerity of Illinois, USA.

Friedel, L., 1979. Improved friction pressure drop correlation for horizontal and vertical two-phase pipe flow, European Two-phase Flow Group Meeting, Paper No. 2, Ispra, Italy (quoted by Whalley (1987)).

Garimellar, S., 2003. Condensation flow mechanisms in microchannels: basis for pressure pressure drop and heat transfer models. In: First International Conference on Microchannels and Minichannels, Rochester, NY, USA, pp. 181–192.

Guo, Z.-Y., Li, Z.-X., 2003. Size effect on microscale single-phase flow and heat transfer. Int. J. Heat and Mass Transfer 46, 149–159.

Heun, M.K., 1995. Performance and optimization of microchannel condensers. Ph.D. Thesis, Univerity of Illinois, USA.

Holman, J.P., 2001. Experimental Methods for Engineers, seventh ed. McGraw-Hill, New York (Chapter 3).

Huber, M., Gallagher, J., McLinden, M., Morrison, G., 1996. NIST Thermodynamic Properties of Refrigerants and Refrigerant Mixtures Database REFPROP, Version 5.1, NIST, USA.

Kandlikar, S.G., 2002. Fundamental issues related to flow boiling in minichannels and microchannels. Experimental Thermal and Fluid Science 26, 389–407.

Kandlikar, S.G., 2003. Microchannels and minichannels—history, terminology, classification and current research needs. In: First International Conference on Microchannels and Minichannels, Rochester, NY, USA, pp. 1–6.

Kandlikar, S.G., Steinke, M.E., Tian, S., Campbell, L.A., 2001. High-speed photographic observation of flow boiling of water in parallel minichannels. In: National Heat Transfer Conference. ASME, New York.

Kim, J.S., 1996, Condensation heat transfer and pressure drop of HFC-134a inside a flat extruded aluminum tube. In: Proceedings of the KSME Autumn Conference, Korea, vol. B, pp. 755–762 (in Korean).

Kim, N.H., Cho, J.P., Kim, J.O., Kim, M.H., Yun, J.H., 1997. Experiments on R-22 condensation heat transfer in small diameter tubes. In: Proceedings of the KSME Autumn Conference, Korea, vol. B, pp. 328–334 (in Korean).

Koyama, S., Kuwahara, K., Nakashita, K., 2003, Condensation of refrigerant in a multi-port channel. In: First International Conference on Microchannels and Minichannels, Rochester, NY, USA, pp. 193–205.

Moser, K., Webb, R.L., Na, B., 1998. A new equivalent Reynolds number model for condensation in smooth tubes. J. Heat Transfer 120, 410–417.

Schnell, G., 1997. Measurement of very small liquid flows. Experimental Thermal and Fluid Science 15, 406–412.

Shah, M.M., 1979. A general correlation for heat transfer during film condensation inside pipes. Int. J. Heat and Mass Transfer 22, 547–556.

Wang, W.W., Radcliff, T.D, Christensen, R.N., 2002. A condensation heat transfer correlation for millimeter-scale tubing with flow regime transition. Experimental Thermal and Fluid Science 26, 473–485.

Webb, R.L., Ermis, K., 2001. Effect of hydraulic diameter on condensation of R-134a in flat, extruded aluminum tubes. J. Enhanced Heat Transfer 8 (2), 77–90.

Whalley, P.B., 1987. Boiling, Condensation, and Gas-liquid Flow. Clarendon Press, Oxford. p. 58.

Wilson, E.E., 1915. A basis for rational design of heat transfer apparatus. Transactions of ASME 37, 47–70.

Yan, Y., Lin, T., 1999. Condensation heat transfer and pressure drop of refrigerant R-134a in a small pipe. Int. J. Heat and Mass Transfer 42, 697–708.

Yang, C., Webb, R.L., 1996. Condensation of R12 in small hydraulic diameter extruded aluminum tubes with and without micro-fins. Int. J. Heat and Mass Transfer 39, 791–800.